Wang, Z., Friedrich, C., Hagemann, S.C., Korte, W.H., Goharani, N., Cording, S., Eberl, G., Sparwasser, T., Lochner, M.

Regulatory T cells promote a protective Th17-associated immune response to intestinal bacterial infection with C. rodentium

(2014) Mucosal Immunology, 7 (6), pp. 1290-1301.

Regulatory T cells promote a protective Th17 associated immune response to intestinal bacterial infection with *C. rodentium*

Zuobai Wang[1], Christin Friedrich[1], Stefanie C. Hagemann[1], Wilhelm H. Korte[1], Naghmeh Goharani[1], Sascha Cording[2], Gérard Eberl[2], Tim Sparwasser[1*] and Matthias Lochner[1*]

[1] Institute of Infection Immunology, TWINCORE, Centre for Experimental and Clinical Infection Research; a joint venture between the Medical School Hannover (MHH) and the Helmholtz Centre for Infection Research (HZI), Hannover, Germany;

[2] Institut Pasteur, Lymphoid Tissue Development Unit, 75724 Paris, France.

* contributed equally

Correspondence:

Dr. Matthias Lochner

Institute of Infection Immunology, TWINCORE, Centre for Experimental and Clinical Infection Research

Feodor-Lyner-Str. 7, 30625 Hannover, Germany

Telephone: +49 (0)511 220027202

E-mail address: Matthias.lochner@twincore.de

Disclosure: The authors declare no conflict of interests

ABSTRACT

Intestinal infection with the mouse pathogen *Citrobacter rodentium* induces a strong local Th17 response in the colon. While this inflammatory immune response helps to clear the pathogen, it also induces inflammation-associated pathology in the gut and thus has to be tightly controlled. In this project we therefore studied the impact of $Foxp3^{+}$ regulatory T cells (Treg) on the infectious and inflammatory processes elicited by the bacterial pathogen *C. rodentium*. Surprisingly, we found that depletion of Treg by diphtheria toxin in the $Foxp3^{DTR}$ (DEREG) mouse model resulted in impaired bacterial clearance in the colon, exacerbated body weight loss and increased systemic dissemination of bacteria. Consistent with the enhanced susceptibility to infection, we found that the colonic Th17 associated T cell response was impaired in Treg depleted mice, suggesting that the presence of Treg is crucial for the establishment of a functional Th17 response after infection in the gut. As a consequence of the impaired Th17 response, we also observed less inflammation-associated pathology in the colons of Treg depleted mice. Interestingly, anti-interleukin (IL)-2 treatment of infected Treg depleted mice restored Th17 induction, indicating that Treg support the induction of a protective Th17 response during intestinal bacterial infection by consumption of local IL-2.

INTRODUCTION

T-helper cell (Th) 17 cells are central to host protection against a wide spectrum of pathogens, especially at mucosal surfaces.[1] Th17 cells express the pro-inflammatory cytokine interleukin (IL)-17 which promotes the generation and recruitment of neutrophils[2], and IL-22[3, 4], which synergizes with IL-17 in the activation of epithelial defense through the expression of anti-bacterial proteins and peptides.[5] The highest proportions of Th17 cells are found in the intestine[6] and the enrichment of these cells in this organ suggests a role for these cells in mucosal homeostasis and more specifically, in the containment of the vast local microbiota. However, sustained activation of Th17 cells can lead to inflammation-associated immunopathology and pathogen-induced Th17 responses have thus to be tightly controlled. Interestingly, Th17 cells and regulatory T cells (Treg) expressing the forkhead box P3 transcription factor (Foxp3) show basic developmental similarities, such as the potential to differentiate in the presence of transforming growth factor beta (TGFβ).[7-11] The presence of a proinflammatory cytokine milieu however favors the development of Th17 cells[11] and the reciprocal relationship between the induction of Th17 cells and Treg suggest that a delicate balance between these T cell lineages is necessary for a viable immunological homeostasis[7, 12]. This is further corroborated by the fact that $Foxp3^+$ cells co-expressing the Th17 "master" transcription factor retinoic acid related orphan receptor gamma t (RORγt) are especially enriched in the intestine[6, 13], where they are induced by the complex microflora[14] and believed to play an important role for the equilibrium between inflammatory Th17 and regulatory Treg.[6, 14] It was in that respect surprising to find that $Foxp3^+$ Treg can promote the induction of a Th17 response *in vitro*, as well as *in vivo* in an infection model with the fungal pathogen *Candida albicans*.[15, 16] This unexpected property of Treg was explained by the ability of Treg to consume local IL-2 and, by lowering the levels of this cytokine, to relieve its inhibiting function on Th17 development.[17]

Given the special relationship between Th17 cells and Treg in the gut with its complex environment containing high loads of commensal microbes, we queried how Treg may influence on the development of an immune response against a bacterial intestinal infection. Using an infection model with the Th17-inducing pathogen *Citrobacter rodentium*[9], we show in this study that the absence of Treg during the initial phase of infection impairs bacterial clearance, the induction of a protective Th17 response and leads to enhanced bacterial dissemination to systemic sites. This demonstrates that Treg can help to establish an effective Th17 response in the gut environment, although this comes at the cost of (transient) immunopathology at the site of infection.

RESULTS

Treg depletion enhances susceptibility towards intestinal infection with *C. rodentium*

To assess the role of Foxp3$^+$ Treg during infection with the gut pathogen *C. rodentium*, we used DEREG mice which express the high affinity diphtheria toxin receptor under the control of the Foxp3 promoter and therefore allow efficient depletion of Treg by diphtheria toxin (DT) treatment.[18] We first confirmed that DT treatment efficiently depleted Treg in the intestine and gut associated lymphoid tissues (GALT). To this end, we treated DEREG mice for two consecutive days after infection with *C. rodentium* with DT and isolated cells from different organs on the third day. We found that in the small intestine, colon, mesenteric lymph nodes (mLN) and Peyer's patches (PP), the Treg frequency was reduced by 85-90%, similar to the reduction levels typically seen in systemic organs like the spleen (**Supplementary Figure 1**). Since Treg start to re-appear around 5-7 days after depletion[19], we performed two rounds of DT-mediated Treg depletion at days 0, 1 and days 7, 8 post-infection (p.i.) with *C. rodentium* (**Supplementary Figure 2a**). Treg frequencies assessed in the blood on the next day after each round of depletion showed reductions of more than 95% after the first round of depletion, and still between 70-80% after the second round of depletion (**Supplementary Figure 2b and c**), indicating that efficient Treg depletion is feasible during the early phase of *C. rodentium* infection.

After having confirmed the feasibility of Treg depletion in *C. rodentium* infection using the DEREG model, we investigated the influence of Treg cell depletion on the severity of infection. While all control mice (PBS treated DEREG mice or DT treated WT mice) were able to survive the infection and showed only modest changes in body weight, Treg depleted mice showed a significant drop in body weight starting from day 7-9 (**Figure 1a**) and high mortality (around 60%) occurring between days 9-12 p.i. (**Figure 1b**). This enhanced susceptibility of Treg depleted mice was accompanied by a markedly increased amount of *C. rodentium* in the feces of the mice (**Figure 1c**).

To monitor the kinetics in bacterial load in more detail, a strain of *C. rodentium* expressing luciferase was used to enable whole body *in vivo* imaging.[20] In accordance with previous studies, the signal of bioluminescence diminished one day after inoculation. Later, the intensity of bioluminescence signal increased from day 1 to 5 in control as well as Treg depleted mice. In control mice, the bioluminescent signal peaked at around day 5 p.i. and decreased afterwards below detection limit on day 11 p.i (**Figure 1d**). Further analysis confirmed that WT controls were able to clear the pathogen after three weeks of infection (**Figure 1e**). In contrast, the bioluminescent signal steadily increased in Treg depleted mice until day 11 p.i., indicating that these mice were impaired in the control of bacterial infection (**Figure 1d**). However, Treg-depleted mice that survived were able to eventually clear the infection, although with a delayed kinetic compared to control animals (**Figure 1e**). Together, these data suggest that depletion of Treg rendered the hosts more susceptible to *C. rodentium* infection.

Treg depletion leads to an impaired Th17 response at the site of mucosal infection

It has recently been demonstrated that innate lymphoid cell (ILC) populations producing the cytokine IL-22 are critical for host protection during the early phase of *C. rodentium* infection.[21, 22] To assess whether Treg depletion impacts on the function of ILC during the early phase of infection, we determined the frequency of IL-22 producing RORγt$^+$ ILC in the colon of Treg depleted mice on day 6 after infection. As shown in **Supplementary Figure 3**, we could detect a substantial frequency of IL-22 producing ILCs in the colon, however with no significant differences between control and Treg depleted mice. Also, in accordance with the infection kinetics shown in **Figure 1d**, there was no difference in the bacterial burden in the feces at this time point (**Figure 1e** and data not shown). This indicates that Treg have no influence on the function of ILC during the early phase of intestinal infection with *C. rodentium*. In contrast, we observed a striking defect in Th17 cell induction in Treg depleted

mice at the peak of the adaptive immune response between day 9-12, when these animals started to become moribund. At this time point, the frequency of IL-17 producing T cells in the lamina propria of the colon was reduced by more than 50% (**Figure 2a**). Interestingly, while the frequency of Interferon (IFN)-γ single producing Th1 cells was not significantly affected (**Figure 2a**), IL-17/IFN-γ double producers were also clearly reduced in Treg depleted mice (**Figure 2a**). Recently, Basu et al. also demonstrated an important role for $CD4^+$ T cell derived IL-22 for host protection against enteropathogenic bacteria.[23] When we analyzed for the frequency of IL-22 producing T cells, we observed a significant reduction in the frequency of IL17/IL-22 double producing, but not in the IL-22 single producing $CD4^+$ T cells after Treg depletion (**Figure 2b**). In addition, we found that this cytokine was significantly reduced on the protein as well as on the transcription level in Treg depleted mice in anti-CD3 stimulated colonic lamina propria lymphocytes (LPL) (**Figure 2c and d**). Similarly, the expression levels of other Th17-associated factors like IL-17F, IL-23r and CCR6 were significantly reduced in restimulated colonic LPL from Treg depleted mice (**Figure 2d**). Further analysis by FACS or RT-PCR from sorted $CD4^+$ colonic T cells suggested that the observed reduction of theses factors in the mixed LPL fraction could mainly be attributed to the $CD4^+$ T cell pool (**Supplementary Figure 4a-c**). While there was only a trend towards less IFN-γ expression in the mixed LPL fraction of Treg depleted mice (Figure 2d), a clear reduction in the expression level of this cytokine was observed in the sorted $CD4^+$ colonic T cells from Treg depleted mice (**Supplementary Figure 4c)**

Together, these data illustrate that the Th17 associated immune response in the colon is dramatically impaired in the absence of Treg cells. Interestingly, we did not observe any impact on the frequency of Th17 cells in the mesenteric lymph nodes or the spleen (**Supplementary Figure 5**), suggesting that the effect of Treg depletion on the Th17 response is restricted to the mucosal site of infection.

Treg depletion impairs neutrophil recruitment to the gut and leads to an enhanced systemic bacterial dissemination

Through secretion of IL-17A and IL17F, Th17 cells can directly induce the recruitment of neutrophils, leading to enhanced clearance of *C. rodentium*[24, 25] and, in concert with IL-22, stimulate the intestinal epithelium to produce antimicrobial proteins and peptides like Reg3γ, Reg3β and β-defensins, which play a crucial role for the maintenance of the epithelial barrier function of the gut.[5, 26, 27] Since we found that Treg absence impaired the Th17 cell response in our system, we next investigated whether this would also affect the downstream recruitment of neutrophils and the level of antimicrobial protein/peptide expression in the gut. Although we did not observe major differences in the expression of Reg3γ and β-defensins 1and 4 (**Supplemental Figure 6**), we found that the recruitment of neutrophils to the colon was clearly impaired after Treg depletion (**Figure 3a**).

Besides its important impact on bacterial clearance through the IL-17-neutrophil axis, it was also suggested that the intestinal Th17 response is important for the effective restriction of bacterial dissemination from the gut.[28] Therefore, we next investigated whether Treg depletion would also affect *C. rodentium* containment to the colon. Live *in vivo* bioluminescence imaging on day 9 p.i. clearly suggested that in contrast to infected WT mice, bacterial colonization in Treg depleted mice was not restricted to the rectal part of the colon as expected[29], but extended to other parts of the gut and internal organs (**Figure 3b**). Direct analysis of the intestine on day 11 after infection revealed high bioluminescent signals in the colon of Treg depleted mice, while the *C. rodentium* derived bioluminescent signal already dropped below the detection limit in the gastrointestinal tract of control mice (**Figure 3c**). As already suggested by live *in vivo* imaging, colonization with *C. rodentium* was not restricted to the colon, but was also detected in the small intestine of Treg depleted mice (**Figure 3c**). Taken together, we conclude that after Treg depletion and the consequent loss of an Th17 associated immune response, the pathogen can expand in parts of the gastrointestinal tract that

are usually not colonized. In addition, a strong bioluminescent signal was also detectable in the livers of Treg depleted mice, while it was below the detection limit observed in control mice (**Figure 3d**). The enhanced bacterial load in this organ in Treg depleted mice was further validated by counting the bacterial CFUs (**Figure 3e**), together showing that Treg depletion resulted in impaired pathogen containment to the colon and elevated systemic bacterial spread.

Reduced immunopathology in the colon of Treg depleted mice

Oral infection with *C. rodentium* induces in WT C57BL/6 mice a transient immunopathology in the colon characterized by an acute colitis, hyperplasia of the colonic crypts and disruption of the normal colonic architecture.[30] This is accompanied by infiltration of inflammatory leukocytes, mainly consisting of $CD4^+$ T cells[31] into the colonic mucosa peaking at around day 10-14 p.i. While this T cell response is essential for host defense against *C. rodentium*, it also mediates much of the tissue pathology and disease symptoms that occur during infection.[31, 32] In accordance with these studies, we found a pronounced hyperplasia, inflammatory cellular infiltration in the mucosa and submucosa, as well as local epithelial injury (**Figure 4**, red stars) in the colon of WT mice on day 12 after infection. Although Treg depleted mice showed similar signs of colon crypt hyperplasia (**Figure 4**, red arrows), suggesting that the turnover of epithelial cell layer was uninfluenced by Treg cell depletion, we observed significantly less cellular infiltration and signs of tissue structure destruction in Treg depleted mice compared to infected WT controls (**Figure 4**). These results thus implicate that Treg depletion during the course of *C. rodentium* infection, rather than leading to enhanced immunopathology as expected, results in less inflammation despite enhanced numbers of infiltrating bacteria. It is probably also in this case as a direct consequence of the impaired Th17 associated immune response in the colon of the Treg depleted mice.

IL-2 neutralization restores colonic Th17 induction in Treg depleted mice

Experimental modeling of the IL-2 signaling network recently revealed that Treg and activated T helper cells compete for local IL-2. Hence, one mechanism how Treg influence on the development of T helper cells responses is by depriving T helper cells of their IL-2.[33] Since IL-2 can inhibit the differentiation of Th17 cells[17], this implicated that Treg might promote colonic Th17 induction after *C. rodentium* infection by local IL-2 consumption. To directly test this hypothesis, we treated Treg-depleted mice with a combination of anti-IL-2 monoclonal antibodies clones JES6-1 and S4B6, a regimen that has been shown to efficiently neutralize the *in vivo* function of IL-2.[34] Intriguingly, anti-IL-2 mAb treatment restored the frequency of IL-17$^+$ and IL-17$^+$IFNγ^+ CD4$^+$ T cells to a level comparable to that in the colons of DT-treated WT controls and also increased the cellular infiltration in the colon of Treg depleted mice (**Figure 5a and b**), indicating that Treg indeed can regulate the induction of the local Th17 response in the colon of *C. rodentium* infected mice by IL-2 consumption. However, further analysis of the downstream effects of IL-17 revealed that the antibody mediated IL-2 neutralization failed to restore the recruitment of neutrophils to the colon of Treg depleted mice (**Figure 5c**). Accordingly, anti-IL-2 mAb treated, Treg depleted mice also failed to clear the pathogen as effectively as WT controls (**Figure 5d**). This discrepancy might be explained by the fact that despite the observed induction of Th17 cells, the total number of IL-17 producing cells per colon was still significantly reduced in anti-IL-2 mAb treated mice (**Figure 5e**). Interestingly, our data suggest that although IL-2 can block the initial Th17 induction, it is still instrumental for sufficient expansion of these cells at later time points.

Nevertheless, IL-2 has complex pleiotropic effects on the homeostasis and activation of the immune system. In our model, IL-2 neutralization already leads to an enhanced systemic Th1 response in infected WT controls (Supplementary Figure 7). Therefore, the failure to completely restore the phenotype might in addition be attributed to other systemic effects of anti-IL-2 treatment.

DISCUSSION

Foxp3$^+$ regulatory T cells are essential for immunological tolerance and homeostasis. Loss-of-function of this transcription factor leads to uncontrolled T-effector cell responses associated with clinical features of systemic autoimmunity in mice and men.[35] While this underscores the importance of Treg for the maintenance of the immunological balance during steady-state conditions, their role during the immune response against acute infections is poorly understood.[36]

In this study, we show that Treg play an important role in the induction of a protective Th17 associated immune response against the gut specific bacterial pathogen *C. rodentium*. These findings might seem counter intuitive at the first glance, since experimental manipulation of Treg using either methods of depletion or expansion of these cells have consistently shown that Treg rather constrain host defense following infections with bacterial and viral pathogens.[37-39] However, our data illustrate the special relationship between Treg and T-effector cells of the Th17 lineage and are in agreement with previous studies that have shown the capacity of Treg to promote IL-17A induction in CD4$^+$ T cells.[15, 16] In addition, a recent report by Moore-Connors et al. demonstrated that Treg can also have a Th17-promoting effect during genital infections with *Chlamydia muridarum*. In accordance with our data, antibody mediated depletion of CD25$^+$ Treg impaired the downstream recruitment of neutrophils and reduced the local inflammatory response.[40] However, the underlying mechanism was not addressed in this study.

We and others have recently shown that CD4$^+$ T cells simultaneously expressing the Th17 lineage marker RORγt and the Treg marker Foxp3 exist under normal homeostatic as well as inflammatory conditions in the gut.[6, 13] Although the *in vivo* function of these cells is still unclear, they have the potential to develop into Foxp3$^+$/RORγt$^+$ IL-17 producing cells.[41] Thus, in our DEREG model, Foxp3$^+$IL-17$^+$ cells would also express the diphtheria toxin receptor (DTR) and be subjected to DT-mediated depletion. Nevertheless, Foxp3$^+$IL-17$^+$ cells only

comprise of less than 1% of all IL-17 producing T cells in the colon after *C. rodentium* infection (data not shown), making it highly unlikely that the depletion of these cells contributed significantly to the phenotype described here.

Intriguingly, Treg depletion strongly affected Th17 development at the site of bacterial infection. Moreover, the frequency of IL-17$^+$IFN-γ^+ double producers was clearly diminished after Treg depletion, suggesting a direct developmental relationship between the classic Th17 cells and IL-17$^+$IFN-γ^+ Th cells, as has been shown for the inflammatory response during experimental autoimmune encephalomyelitis using an IL-17 fate mapping strategy.[42] Notably, IL-17$^+$IFN-γ^+ cells have been associated with enhanced reactivity and pathological potential in the intestine[43-45] and studies using IFN-γ deficient mice suggest an important role for this cytokine in the defense against *C. rodentium* infection.[46] It is tempting therefore to speculate that the IL-17$^+$IFN-γ^+ Th cells not only play a key role for the bacterial clearance, but also contribute essentially to the tissue pathology observed in this model. Although our data indicate that the frequency of IFN-γ producing T cells is less affected by Treg depletion, the classical Th1 response might also be impaired in terms of total Th1 cell numbers.

IL-22 plays a crucial role for host protection at mucosal barrier sites and mice deficient for this cytokine succumb rapidly to infection with *C. rodentium.*[22, 47] During the early phase of infection, most IL-22 is produced by RORγt expressing ILC in an IL-23 dependent manner.[21, 22] Our data indicate that this early ILC mediated immune response is not affected by the absence of Treg, although we can not rule out an effect on other RORγt-negative ILC populations in this model. Nevertheless, T cell derived IL-22 was significantly reduced after Treg depletion at the later stage of infection as a direct consequence of the impaired Th17 induction in Treg depleted mice, rather than an effect on the recently described IL-22$^+$ IL-17$^-$ Th22 cells.[23] As we did not observe any differences in the expression levels of the antimicrobial peptides and proteins that were addressed in our study, it remains to be further

analyzed whether the impaired IL-22 response contributes to the enhanced susceptibility of Treg depleted mice to *C. rodentium* infection in our model.

Foxp3$^+$ Treg express high levels of the IL-2 receptor α chain CD25 and, while they are highly dependent on the presence of IL-2 for their survival and suppressive function, they can not produce this cytokine by themselves.[48] Thus, they efficiently can take up IL-2 present in their environment and this property is thought to play an important role for their regulatory function on T effector cells[34, 49, 50] and, as recently reported, also on NK cells.[51, 52] In their reports, Pandiyan and Chen suggested that consumption of IL-2 by Treg is the main mechanism by which Treg support the induction of Th17 cells.[15, 16] Our data now indicate that this mechanism is also operational under highly infectious conditions in the gut. Of note, IL-2 neutralization in the absence of Treg resulted in restored Th17 cell frequencies at the local site of infection, but also resulted in systemic side effects during infection, showing that IL-2 neutralization is not a therapeutic option to enhance anti-bacterial immune responses *in vivo*. More importantly, total numbers of colonic IL-17 producing T cells were still reduced after anti-IL-2 treatment of Treg depleted mice. This failure to fully restore the phenotype might be explained by a more complex action of IL-2 on Th17 cells. As outlined by the studies of Pandiyan and Chen, the inhibitory effect of IL-2 on the Th17 development is likely to be only functional during the early induction period.[15, 16] In addition, IL-2 has shown to be important for the expansion of Th17 cells, once generated.[53] Considering that in our experimental approach IL-2 is neutralized during the whole period of the infection, we might therefore not only induce the initial formation of Th17 cells, but also prevent their expansion during the later phase and, as a consequence, the subsequent recruitment of neutrophils.

While anti-IL-2 treatment of Treg depleted mice did not restore the recruitment of neutrophils to the colon and also had no impact on bacterial load in these mice, we still observed an increase in cellular infiltration into the colon. Whether this reflects the small increase in the

amount of Th17 cells or if other cells types are recruited after IL-2-neutralization is however not clear and remains to be studied.

Finally, the question remains if this surprising capacity of Treg to support local Th17 induction is of any physiological relevance? Considering the high frequencies of Treg in mucosal tissues, especially the colon (Supplementary Figure 1 and unpublished observations) under normal homeostatic conditions, this might favor the induction of an appropriate Th17 immune response at the initial phase of a mucosal infection. Thus, the ability of Treg to promote Th17 cells might represent an important mechanism of immune regulation especially in the gut.

METHODS

Mice and bacterial strains. C57BL/6 mice were purchased from Charles River. BAC transgenic DEREG mice have been described previously[18]. All control mice used in experiments were nontransgenic litter of heterogenic DEREG breeding pairs. Mice were bred and maintained under specific pathogen free condition in our animal facilities (TWINCORE, Hannover, Germany; Helmholtz center for infection research, Braunschweig, Germany). All animals used in experiments were of approximate 7 to 10 weeks with matched gender. All animal experiments were performed in compliance with the German animal protection law (TierSchG BGBl. I S. 1105; 25.05.1998). The mice were housed and handled in accordance with good animal practice as defined by FELASA and the national animal welfare body GV-SOLAS. All animal experiments were approved by the Lower Saxony Committee on the Ethics of Animal Experiments as well as the responsible state office (Lower Saxony State Office of Consumer Protection and Food Safety) under the permit numbers 33.9-42502-04-10/0244. *Citrobacter rodentium* (previously known as *Citrobacter freundii*, biotype 4280) strain ICC 180 expressing bioluminescent signal was described previously by Wiles et al. [20].

Reagents and antibodies. The following antibodies were purchased from eBioscience: PerCP Cyan 5.5-conjugated anti-mouse CD4 (clone: RM 4-5), PE-Cyan 7-conjugated anti-mouse CD4 (clone: GK 1.5), eFluor 660-conjugated anti-mouse CD4 (clone: GK1.5), PE-conjugated anti-mouse CD3 (clone: 145-2C11), APC eFluor 780-conjugated anti-mouse CD3 (clone: 17A2), functional grade anti-mouse CD3 (clone: 145-2C11), APC eFluor 780-conjugated anti-mouse TCRbeta (clone: H57-597), Biotin-conjugated anti-mouse TCRbeta (clone: H57-597), eFluor 450-conjugated anti-mouse Foxp3 (clone: FJK-16S), PE-conjugated anti-mouse RORγt (clone: B2D), APC-conjugated anti-human/mouse RORγt (clone: AFKJS-9), Alexa 647-conjugated anti-mouse IFNγ (clone: XMG1.2), PE Cyan 7-conjugated anti-mouse IFN-γ

(clone: XMG1.2), APC-conjugated anti-mouse IL-17A (clone: eBio17B7), PE-conjugated anti-mouse IL-17A (clone: eBio17B7), eFluor 660-conjugated anti-mouse IL-17F (clone: eBio18F10), PE-conjugated anti-mouse IL-22 (clone: 1H8PWSR), PerCP eFluor 710 conjugated anti-mouse IL-22 (clone: 1H8PWSR), APC-conjugated anti-mouse CD11b (clone: M1/70), and PE-conjugated anti-mouse CD11c (clone: N418); the following antibodies are from Biolegend: PE Cyan 7-conjugated anti-mouse Ly-6G (clone: 1A8), Alexa 647-conjugated anti-mouse IL-22 (clone: Poly5164); the following antibodies are from BD Biosciences: Alexa Fluor 647-conjugated anti-mouse CCR6 (clone: 140706), APC-conjugated anti-Biotin, and Biotin-conjugated anti-mouse Ly-6C (clone: AL-21). *Diphtheria toxin* (isolated from *Corynebacterium diphtheriae*) was obtained from Sigma-Aldrich. Anti-IL-2 mAb (clone JES1-4 and S4B6, blocking high affinity and low affinity IL-2R binding sites, respectively) was purchased from BioXcell.

***C. rodentium* infection and treatment.** *C. rodentium* strain ICC180 was used for all of the experiments. Mice were orally gavaged with $1x10^{10}$ CFU of *C. rodentium* in a total volume of 100 μl of PBS. On Day 0, 1, 7 and 8 post infection, mice received 50 ng/g body weight of *Diphtheria toxin* in 100 μl of PBS i.p. For *in vivo* IL-2 neutralization,, 200 μg of anti-IL-2 (1:1 mixture of clone JES1-4 and S4B6) mAb in 100 μl of PBS or blank control (100 μl of PBS) was injected i.p. on daily basis.

Colony counts of *C. rodentium*. For bacterial burden in colonic feces, stools from infected mice were collected into a preweighed Luria Bertani medium containing tube. Feces were then weighed, homogenized and titrated. Series of feces dilution were added on MacConkey Agar and then cultured at 37°C for one day before counting. Baterial burden was calculated after normalization to the weight of stool. For bacterial burden in livers, organs were homogenized in 1 ml LB medium. Homogenous liquids were further titrated, plated on

MacConkey Agar, and incubated at 37°C for two days before counting.

***In vivo* Imaging.** Mice were anesthetized with isoflurane (Baxter) carried in 2% O_2 and placed in a supine position in a chamber for imaging with an IVIS Spectrum CT (PerkinElmer). Photon flux was further analyzed by using Living Image 4.3.1 Software (PerkinElmer). Uninfected DT-i.p. injected non-transgenic mice were served as baseline controls. After infection with bioluminescent *C. rodentium* strain ICC180, whole-body images or dissected organs were taken at a binning factor of 8 over 5 sec to 3 min at the indicated time points during infection. Luminescence emitted from region of interest (ROI) with the same size in individual mouse was quantified as total flux and pseudocolor images representing intensity from bacteria-derived luminescence were generated. For detection of 3 dimensional bioluminescent signal, anesthetized mice were first scanned by computed tomography (CT) under the mode of medium resolution and then *C. rodentium*-derived bioluminescent signal was excited under the wavelength of 489 nm and imaged at a binning factor of 8 over 5 sec to 1 min.

Isolation of Epithelial cells and Lamina Propria Cells. Colons were isolated from animals and remaining feces were removed. The colon was cut into several pieces and was incubated in 15 ml of ice-chilled 0.5 mM EDTA for 30 min at 4°C and then rinsed extensively with PBS (Ca^{2+}/Mg^{2+} free). Epithelial cells were pooled to from the supernatant after each round of rinsing and collected by centrifugation at 250 x g for 10 min at 4°C. Collected epithelial cells were resuspended in 1 ml of TRIzol (life technologies) for further RNA extraction. After removal of any residual epithelium, tissues were cut into small pieces and incubated in DMEM medium (Life/Gibco) containing 1 mg/ml collagenase D (Roche) and 0.1 mg/ml DNase I (Roche) for three rounds of 30 min at 37°C. Tissue suspensions were then passed through 100 μm mesh, pelleted, resuspended in a 40% isotonic Percoll solution (GE

Healthcare), and underlain with an 80% isotonic Percoll solution. After centrifugation at 900 x g for 20 min at room temperature, lamina propria lymphocytes (LPLs) were yielded from the interface of 40-80% Percoll solution. Cells were washed once with PBS-F (PBS containing 2% FCS) and then used for analyses.

Flow Cytometry. For cell surface marker staining, cells were preincubated with 1% Fc-block in PBA (0.25% BSA, 0.02% sodium azide in PBS) at 4°C for 10 min, and then washed and incubated in indicated mAb conjugates for 20 min in a total volume of 50 µl of PBA. For intracellular cytokine/transcription factor staining, cells were restimulated for 4 h in complete RPMI medium (Life/Gibco) in the presence of 100 ng/ml phorbol 12-myristate 13-acetate and 1 µg/ml ionomycin (both from Sigma-Aldrich). For the last 2 h, 1 x Brefeldin A (Sigma-Aldrich) was added to the cultures. After live/dead staining with aqua fluorescent reactive dye (Invitrogen) and surface staining for CD4, CD3, and/or TCRβ, cells were fixed in 100 µl of Fixation/Permeabilization concentrate and diluent (eBioscience) at 4°C for 20 min. Intracellular staining was performed in 50 µl of permeabilization-solution (1% saponin in PBA) with anti-Foxp3, anti-RORγt, anti-IL-17, and anti-IFN-γ, anti-IL-22, anti-IL-17F. Samples were acquired on CyAn ADP (Beckman Coulter) or LSR II (BD Biosciences) and analyzed with FlowJo software9.4 (Tree Star).

mRNA Isolation and quantitative real time-PCR. Isolated LPLs were either directly incubated or FACS-sorted according to the co-expression of surface marker CD3 and CD4 (MoFlo XDP, Beckman Coulter) and then cultured in complete RPMI medium in the presence of 0.5 µg/ml anti-CD3 mAb at 37°C for 24 h. RNA was obtained from cultured LPLs with Qiagen RNeasy Micro Kit (Qiagen) and further quantified using NanoDrop-1000 spectrophotometer (Peqlab). For epithelial cell RNA extraction, cells were collected in 1 ml of TRIzol and RNA was further isolated according to the manufacturer's manual and quantified

using NanoDrop-1000 spectrophotometer. cDNA was afterwards reverse transcribed with 0.1 µg of RNA from LPLs or 1µg of RNA from epithelial cells using superscript® III reverse Transcriptase (Life Technologies). Real-time PCR for the study of *Il17a*, *Il17f* , *Ifng*, *Il22*, *Il23r*, and *Ccr6* mRNA expression (primers from Qiagen) or *Reg3g* (obtained from Eurofins MWG Operon; forward strand: CCTTCCTCTTCCTCAGGCAAT; reverse strand: TAATTCTCTCTCCACTTCAGAAATCCT), *β-defensin1* (obtained from Eurofins MWG Operon; forward strand: AGGTGTTGGCATTCTCACAAG; reverse strand: GCTTATCTGGTTTACAGGTTCCC) and *β-defensin4* (obtained from Eurofins MWG Operon; forward strand: GCAGCCTTTACCCAAATTATC; reverse strand: ACAATTGCCAATCTGTCGAA) was carried out with iQ™ SYBR® green supermix (Bio-Rad). Expressions of target genes were normalized to *Actinb* (Qiagen). Samples were analyzed on a LightCycler 480 II (Roche).

Cytokine production detection by enzyme-linked immunosorbent assay. The cytokine production assay Culture supernatant of each sample was collected after 24 h incubation of LPLs in complete RPMI medium containing 0.5 µg/ml anti-CD3 mAb at 37°C. Cytokine productions were detected by a IL-22 kit performed according to the manufacturer's instructions (R&D) and data acquired with a Synergy II (Biotek).

Histopathologic scoring. To assess tissue pathology, we used a scoring system adapted from a previously described scoring system [54]. In brief, whole colons were placed in a shape of Swiss roll, embedded in paraffin and further cut 5 µm in thickness. Tissues were then stained with haematoxylin and eosin (H&E) and were examined by a trained blinded observer. Tissue sections were assessed for epithelial hyperplasia (score based on percentage above the height of the control where 0= no change; 1=1–50%; 2=51–100%; 3=.100%; epithelial integrity (0= no change; 1= mild epithelial ulceration and crypt destruction; 2= moderate epithelial

ulceration and crypt destruction; 3= severe epithelial ulceration with crypt destruction); mononuclear cell infiltration (0= none; 1= mild; 2= moderate; 3= severe). The maximum score that could result from this scoring was 9. Samples were imaged under microscope (Carl Zeiss, Inc.) and progressed with software Nuance 2.10.0 (Carl Zeiss, Inc.).

Statistics. Results represent the mean ± S.E.M.. Statistics was analyzed by Student's t test or Mann-Whiteney U test unless additionally indicated. *<0.05, **<0.01, ***<0.001.

SUPPLEMENTAL MATERIAL is linked to the online version of the paper

ACKNOWLEDGEMENTS

We thank M. Hornef, F. Puttur, P. Ghorbani for discussions and critical reading of the manuscript; S. Wiles for providing us with *C. rodentium* ICC180 and F. Kruse and M. Gohmert for their excellent technical help. We would like to acknowledge the assistance of the Cell Sorting Core Facility of the Hanover Medical School supported in part by Braukmann-Wittenberg-Herz-Stiftung and Deutsche Forschungsgemeinschaft. This work was supported by grant LO1415/2-1 from the Deutsche Forschungsgemeinschaft (DFG.), the Novartis Foundation for therapeutic research, the TUI-Foundation, the Hannover Biomedical Research School (HBRS), Helmholtz International Research School for Infection Research (HIRSIB), and the Center for Infection Biology (ZIB) with a DEWIN stipend to Z.W. This work is part of the thesis of Z.W.

DISCLOSURE

The authors declare no conflict of interests.

REFERENCES

1. Khader SA, Gaffen SL, Kolls JK. Th17 cells at the crossroads of innate and adaptive immunity against infectious diseases at the mucosa. *Mucosal Immunol* 2009; **2**(5)**:** 403-411.

2. Weaver CT, Hatton RD, Mangan PR, Harrington LE. IL-17 family cytokines and the expanding diversity of effector T cell lineages. *Annu Rev Immunol* 2007; **25:** 821-852.

3. Kreymborg K, Etzensperger R, Dumoutier L, Haak S, Rebollo A, Buch T *et al.* IL-22 is expressed by Th17 cells in an IL-23-dependent fashion, but not required for the development of autoimmune encephalomyelitis. *J Immunol* 2007; **179**(12)**:** 8098-8104.

4. Zheng Y, Danilenko DM, Valdez P, Kasman I, Eastham-Anderson J, Wu J *et al.* Interleukin-22, a T(H)17 cytokine, mediates IL-23-induced dermal inflammation and acanthosis. *Nature* 2007; **445**(7128)**:** 648-651.

5. Liang SC, Tan XY, Luxenberg DP, Karim R, Dunussi-Joannopoulos K, Collins M *et al.* Interleukin (IL)-22 and IL-17 are coexpressed by Th17 cells and cooperatively enhance expression of antimicrobial peptides. *J Exp Med* 2006; **203**(10)**:** 2271-2279.

6. Lochner M, Peduto L, Cherrier M, Sawa S, Langa F, Varona R *et al.* In vivo equilibrium of proinflammatory IL-17+ and regulatory IL-10+ Foxp3+ RORgamma t+ T cells. *J Exp Med* 2008; **205**(6)**:** 1381-1393.

7. Bettelli E, Carrier Y, Gao W, Korn T, Strom TB, Oukka M *et al.* Reciprocal developmental pathways for the generation of pathogenic effector TH17 and regulatory T cells. *Nature* 2006; **441**(7090)**:** 235-238.

8. Chen W, Jin W, Hardegen N, Lei KJ, Li L, Marinos N *et al.* Conversion of peripheral CD4+CD25- naive T cells to CD4+CD25+ regulatory T cells by TGF-beta induction of transcription factor Foxp3. *J Exp Med* 2003; **198**(12)**:** 1875-1886.

9. Mangan PR, Harrington LE, O'Quinn DB, Helms WS, Bullard DC, Elson CO *et al.* Transforming growth factor-beta induces development of the T(H)17 lineage. *Nature* 2006; **441**(7090)**:** 231-234.

10. Marie JC, Letterio JJ, Gavin M, Rudensky AY. TGF-beta1 maintains suppressor function and Foxp3 expression in CD4+CD25+ regulatory T cells. *J Exp Med* 2005; **201**(7)**:** 1061-1067.

11. Veldhoen M, Hocking RJ, Atkins CJ, Locksley RM, Stockinger B. TGFbeta in the context of an inflammatory cytokine milieu supports de novo differentiation of IL-17-producing T cells. *Immunity* 2006; **24**(2)**:** 179-189.

12. Weaver CT, Hatton RD. Interplay between the TH17 and TReg cell lineages: a (co-)evolutionary perspective. *Nat Rev Immunol* 2009; **9**(12)**:** 883-889.

13. Zhou L, Lopes JE, Chong MM, Ivanov, II, Min R, Victora GD *et al.* TGF-beta-induced Foxp3 inhibits T(H)17 cell differentiation by antagonizing RORgammat function. *Nature* 2008; **453**(7192)**:** 236-240.

14. Lochner M, Berard M, Sawa S, Hauer S, Gaboriau-Routhiau V, Fernandez TD *et al.* Restricted microbiota and absence of cognate TCR antigen leads to an unbalanced generation of Th17 cells. *J Immunol* 2011; **186**(3)**:** 1531-1537.

15. Chen Y, Haines CJ, Gutcher I, Hochweller K, Blumenschein WM, McClanahan T *et al.* Foxp3(+) regulatory T cells promote T helper 17 cell development in vivo through regulation of interleukin-2. *Immunity* 2011; **34**(3)**:** 409-421.

16. Pandiyan P, Conti HR, Zheng L, Peterson AC, Mathern DR, Hernandez-Santos N *et al.* CD4(+)CD25(+)Foxp3(+) regulatory T cells promote Th17 cells in vitro and enhance host resistance in mouse Candida albicans Th17 cell infection model. *Immunity* 2011; **34**(3)**:** 422-434.

17. Laurence A, Tato CM, Davidson TS, Kanno Y, Chen Z, Yao Z *et al.* Interleukin-2 signaling via STAT5 constrains T helper 17 cell generation. *Immunity* 2007; **26**(3)**:** 371-381.

18. Lahl K, Loddenkemper C, Drouin C, Freyer J, Arnason J, Eberl G *et al.* Selective depletion of Foxp3+ regulatory T cells induces a scurfy-like disease. *J Exp Med* 2007; **204**(1)**:** 57-63.

19. Lahl K, Sparwasser T. In vivo depletion of FoxP3+ Tregs using the DEREG mouse model. *Methods Mol Biol* 2011; **707:** 157-172.

20. Wiles S, Clare S, Harker J, Huett A, Young D, Dougan G *et al.* Organ specificity, colonization and clearance dynamics in vivo following oral challenges with the murine pathogen Citrobacter rodentium. *Cell Microbiol* 2004; **6**(10)**:** 963-972.

21. Satoh-Takayama N, Vosshenrich CA, Lesjean-Pottier S, Sawa S, Lochner M, Rattis F *et al.* Microbial flora drives interleukin 22 production in intestinal NKp46+ cells that provide innate mucosal immune defense. *Immunity* 2008; **29**(6)**:** 958-970.

22. Sonnenberg GF, Monticelli LA, Elloso MM, Fouser LA, Artis D. CD4(+) lymphoid tissue-inducer cells promote innate immunity in the gut. *Immunity* 2011; **34**(1)**:** 122-134.

23. Basu R, O'Quinn DB, Silberger DJ, Schoeb TR, Fouser L, Ouyang W *et al.* Th22 cells are an important source of IL-22 for host protection against enteropathogenic bacteria. *Immunity* 2012; **37**(6)**:** 1061-1075.

24. Lebeis SL, Bommarius B, Parkos CA, Sherman MA, Kalman D. TLR signaling mediated by MyD88 is required for a protective innate immune response by neutrophils to Citrobacter rodentium. *J Immunol* 2007; **179**(1)**:** 566-577.

25. Spehlmann ME, Dann SM, Hruz P, Hanson E, McCole DF, Eckmann L. CXCR2-dependent mucosal neutrophil influx protects against colitis-associated diarrhea

caused by an attaching/effacing lesion-forming bacterial pathogen. *J Immunol* 2009; **183**(5)**:** 3332-3343.

26. Sonnenberg GF, Fouser LA, Artis D. Border patrol: regulation of immunity, inflammation and tissue homeostasis at barrier surfaces by IL-22. *Nat Immunol* 2011; **12**(5)**:** 383-390.

27. Ishigame H, Kakuta S, Nagai T, Kadoki M, Nambu A, Komiyama Y *et al.* Differential roles of interleukin-17A and -17F in host defense against mucoepithelial bacterial infection and allergic responses. *Immunity* 2009; **30**(1)**:** 108-119.

28. Ohnmacht C, Marques R, Presley L, Sawa S, Lochner M, Eberl G. Intestinal microbiota, evolution of the immune system and the bad reputation of pro-inflammatory immunity. *Cell Microbiol* 2011; **13**(5)**:** 653-659.

29. Wiles S, Pickard KM, Peng K, MacDonald TT, Frankel G. In vivo bioluminescence imaging of the murine pathogen Citrobacter rodentium. *Infect Immun* 2006; **74**(9)**:** 5391-5396.

30. Luperchio SA, Schauer DB. Molecular pathogenesis of Citrobacter rodentium and transmissible murine colonic hyperplasia. *Microbes Infect* 2001; **3**(4)**:** 333-340.

31. Higgins LM, Frankel G, Douce G, Dougan G, MacDonald TT. Citrobacter rodentium infection in mice elicits a mucosal Th1 cytokine response and lesions similar to those in murine inflammatory bowel disease. *Infect Immun* 1999; **67**(6)**:** 3031-3039.

32. Vallance BA, Deng W, Knodler LA, Finlay BB. Mice lacking T and B lymphocytes develop transient colitis and crypt hyperplasia yet suffer impaired bacterial clearance during Citrobacter rodentium infection. *Infect Immun* 2002; **70**(4)**:** 2070-2081.

33. Busse D, de la Rosa M, Hobiger K, Thurley K, Flossdorf M, Scheffold A *et al.* Competing feedback loops shape IL-2 signaling between helper and regulatory T lymphocytes in cellular microenvironments. *Proc Natl Acad Sci U S A* 2010; **107**(7)**:** 3058-3063.

34. McNally A, Hill GR, Sparwasser T, Thomas R, Steptoe RJ. CD4+CD25+ regulatory T cells control CD8+ T-cell effector differentiation by modulating IL-2 homeostasis. *Proc Natl Acad Sci U S A* 2011; **108**(18)**:** 7529-7534.

35. Mayer CT, Berod L, Sparwasser T. Layers of dendritic cell-mediated T cell tolerance, their regulation and the prevention of autoimmunity. *Front Immunol* 2012; **3:** 183.

36. Berod L, Puttur F, Huehn J, Sparwasser T. Tregs in infection and vaccinology: heroes or traitors? *Microb Biotechnol* 2012; **5**(2)**:** 260-269.

37. Arnold IC, Lee JY, Amieva MR, Roers A, Flavell RA, Sparwasser T *et al.* Tolerance rather than immunity protects from Helicobacter pylori-induced gastric preneoplasia. *Gastroenterology* 2011; **140**(1)**:** 199-209.

38. Loebbermann J, Thornton H, Durant L, Sparwasser T, Webster KE, Sprent J *et al.* Regulatory T cells expressing granzyme B play a critical role in controlling lung inflammation during acute viral infection. *Mucosal Immunol* 2012; **5**(2)**:** 161-172.

39. Zelinskyy G, Dietze KK, Husecken YP, Schimmer S, Nair S, Werner T *et al.* The regulatory T-cell response during acute retroviral infection is locally defined and controls the magnitude and duration of the virus-specific cytotoxic T-cell response. *Blood* 2009; **114**(15)**:** 3199-3207.

40. Moore-Connors JM, Fraser R, Halperin SA, Wang J. CD4(+)CD25(+)Foxp3(+) regulatory T cells promote Th17 responses and genital tract inflammation upon intracellular Chlamydia muridarum infection. *J Immunol* 2013; **191**(6)**:** 3430-3439.

41. Osorio F, LeibundGut-Landmann S, Lochner M, Lahl K, Sparwasser T, Eberl G *et al.* DC activated via dectin-1 convert Treg into IL-17 producers. *Eur J Immunol* 2008; **38**(12)**:** 3274-3281.

42. Hirota K, Duarte JH, Veldhoen M, Hornsby E, Li Y, Cua DJ *et al.* Fate mapping of IL-17-producing T cells in inflammatory responses. *Nat Immunol* 2011; **12**(3)**:** 255-263.

43. Ahern PP, Schiering C, Buonocore S, McGeachy MJ, Cua DJ, Maloy KJ *et al.* Interleukin-23 drives intestinal inflammation through direct activity on T cells. *Immunity* 2010; **33**(2)**:** 279-288.

44. Hue S, Ahern P, Buonocore S, Kullberg MC, Cua DJ, McKenzie BS *et al.* Interleukin-23 drives innate and T cell-mediated intestinal inflammation. *J Exp Med* 2006; **203**(11)**:** 2473-2483.

45. Kullberg MC, Jankovic D, Feng CG, Hue S, Gorelick PL, McKenzie BS *et al.* IL-23 plays a key role in Helicobacter hepaticus-induced T cell-dependent colitis. *J Exp Med* 2006; **203**(11)**:** 2485-2494.

46. Shiomi H, Masuda A, Nishiumi S, Nishida M, Takagawa T, Shiomi Y *et al.* Gamma interferon produced by antigen-specific CD4+ T cells regulates the mucosal immune responses to Citrobacter rodentium infection. *Infect Immun* 2010; **78**(6)**:** 2653-2666.

47. Zheng Y, Valdez PA, Danilenko DM, Hu Y, Sa SM, Gong Q *et al.* Interleukin-22 mediates early host defense against attaching and effacing bacterial pathogens. *Nat Med* 2008; **14**(3)**:** 282-289.

48. Sakaguchi S, Yamaguchi T, Nomura T, Ono M. Regulatory T cells and immune tolerance. *Cell* 2008; **133**(5)**:** 775-787.

49. Kastenmuller W, Gasteiger G, Subramanian N, Sparwasser T, Busch DH, Belkaid Y *et al.* Regulatory T cells selectively control CD8+ T cell effector pool size via IL-2 restriction. *J Immunol* 2011; **187**(6)**:** 3186-3197.

50. Pandiyan P, Zheng L, Ishihara S, Reed J, Lenardo MJ. CD4+CD25+Foxp3+ regulatory T cells induce cytokine deprivation-mediated apoptosis of effector CD4+ T cells. *Nat Immunol* 2007; **8**(12)**:** 1353-1362.

51. Gasteiger G, Hemmers S, Bos PD, Sun JC, Rudensky AY. IL-2-dependent adaptive control of NK cell homeostasis. *J Exp Med* 2013; **210**(6)**:** 1179-1187.

52. Sitrin J, Ring A, Garcia KC, Benoist C, Mathis D. Regulatory T cells control NK cells in an insulitic lesion by depriving them of IL-2. *J Exp Med* 2013; **210**(6)**:** 1153-1165.

53. Amadi-Obi A, Yu CR, Liu X, Mahdi RM, Clarke GL, Nussenblatt RB *et al.* TH17 cells contribute to uveitis and scleritis and are expanded by IL-2 and inhibited by IL-27/STAT1. *Nat Med* 2007; **13**(6)**:** 711-718.

54. Bergstrom KS, Kissoon-Singh V, Gibson DL, Ma C, Montero M, Sham HP *et al.* Muc2 protects against lethal infectious colitis by disassociating pathogenic and commensal bacteria from the colonic mucosa. *PLoS Pathog* 2010; **6**(5)**:** e1000902.

FIGURE LEGENDS

Figure 1 Foxp3$^+$ cell depletion results in enhanced susceptibility of hosts towards infection with *C. rodentium*. DEREG transgenic mice or nontransgenic control littermates (n= 3~5 mice per group) were orally gavaged with *C. rodentium* (luminescent strain ICC180), then injected i.p. with DT or PBS on day 0, 1, 7 and 8 post infection (p.i.). (**a**) Body weight change post infection. One representative shown out of at least five individual experiments with 3-7 mice per group. Data are mean ± S.E.M.. *<0.05. (**b**) Survival curve of *C. rodentium* infected Treg depleted or non-depleted hosts till day 25 post infection. Data are one representative of three individual experiments with 5 mice per group. Statistics are analyzed according to Log-rank (Mantel-Cox) test, *<0.05. (**c**) *C. rodentium* burden in colonic stool day 12 post infection. Data, representing mean, are pooled from at least four individual experiments. **<0.01. (**d**) Serial whole-body imaging of C. rodentium infected DEREG or non-transgenic WT littermates imaged at the indicated days p.i (upper panel). Total flux of i*n vivo C. rodentium*-derived bioluminescent signals in different groups (n= 3 to 4) at different time points (lower panel). Data are shown for one out of 3 individual experiments. Data are mean ± S.E.M.. *<0.05. (**e**) Kinetics of *C. rodentium* burden in the feces collected from Treg depleted or non-depleted hosts till day 25 post infection. Data are one representative of three individual experiments, each with 5 mice per group. Data represent mean ± S.E.M.. *<0.05, **<0.01.

Figure 2 Treg depletion leads to an impaired Th17 response at the site of infection. (**a**) FACS analysis of IFN-γ and IL-17A expression by colonic lamina propria lymphocytes (cLPLs) of mice from different groups 10 to 12 days p.i. FACS plots from one representative out of 3 individual experiments (upper panel, gated on CD3$^+$CD4$^+$ T cells). Data shown in the graphs represent mean, pooled from 3 individual experiments, each with 3 to 5 mice per group (lower panel). ***<0.001. (**b**) FACS analysis of IL-17A and IL-22 expression by cLPLs of mice

from different groups 10 days after *C. rodentium* infection. FACS plots (upper panels, gated on $CD3^+CD4^+$ T cells) are shown for one representative out of 2 individual experiments. Data are pooled from 2 individual experiments (lower panel), each with 2 to 4 mice per group. Data represent mean. ***<0.001 (**c**) 5 x 10^5 isolated cLPLs were restimulated in RPMI complete medium containing 0.5 μg/ml anti-CD3 mAb per well for 24 h at 37 °C. Cell culture supernatants were collected for IL-22 ELISA and (**d**) cells were harvested and analyzed for gene expression by RT-PCR. Gene expression was normalized to expression of *β-actin* and is shown as fold difference. Data represent mean ± S.E.M.. Representative of 3 individual experiments, with 3 mice per group. *<0.05, **<0.01, ***<0.001.

Figure 3 Treg depletion impairs neutrophil recruitment and leads to systemic spreading of *C. rodentium.* (**a**) FACS of $CD11b^+CD11c^-Ly6G^{high}Ly6C^{int}$ colonic lamina propria neutrophils of mice from different groups 10 to 12 days post *C. rodentium* infection. FACS plot one shown for representative out of 3 individual experiments (left panel). Data depicted represents frequencies of colonic $Ly6G^{high}Ly6C^{int}$ neutrophils among $CD11b^+CD11c^-$ cells in mice from different groups (middle panel). Data, shown as mean, represent one representative out of 3 individual experiments, each with 2 to 4 mice per group. Bar chart represents total number of neutrophils in the colons of mice from different groups (right panel). Data, shown as mean ± S.E.M., display one representative of 3 individual experiments. *<0.05. (**b**) Computed tomography scanning image of Treg depleted or non-depleted mice infected with bioluminescent *C. rodentium* on day 9 p.i. (**c**) Whole-gut imaging of DT injected DEREG or wild type littermates after 11 days of infection with *C. rodentium*. (**d**) Whole organ imaging of dissected livers from DT treated DEREG and wild type littermates infected with bioluminescent *C. rodentium* on day 11 p.i. (**e**) *C. rodentium* burden in livers from *C. rodentium* infected and DT treated DEREG or wild type littermates on day 11 p.i.. Data are mean ± S.E.M.. Data are one representative of three (Figure 3b, 3c, 3d, n=3 to 4 mice per

group) or at least four individual experiments (Figure 3e, n=3 to 7 mice per group). *<0.05, **<0.01.

Figure 4 Immunopathology is reduced in the colon of Treg depleted mice. H&E staining of colonic tissues from *C. rodentium* infected and DT treated wild type (WT) littermates and DEREG mice on day 11 p.i. or uninfected DT injected wild type littermates. Red stars indicate severe infiltration and epithelial injury; Red arrows represent crypt hyperplasia. Data represent one individual experiment of at least 3 individual experiments (n=3-5 mice per group). Lower left panel depicts histopathological scoring of colons from *C. rodentium* infected and DT treated DEREG or wild type littermates on day 11 p.i. Data are mean ± S.E.M. from one representative of at least 3 individual experiments (n=3-5 mice per group). *<0.05. Scale bar represents 200 μm.

Figure 5 Anti-IL-2 mAb treatment restores intestinal Th17 cell induction. DEREG or nontransgenic wild type littermates were infected with *C. rodentium* and treated with DT at day 0, 1, 7 and 8 p.i. 200 μg anti-IL-2 mAbs (clone JES4-1 and S4B6) in 100 μl of PBS were i.p. injected on a daily basis until day 9 p.i. and mice were analyzed on day 10 p.i.. (**a**) FACS analysis of IFN-γ and IL-17A expression by cLPLs (upper panel). Graphs of different colonic cell subsets (lower panel). Data are pooled from 3 individual experiments, with 2 to 3 mice per group. Data represents mean. *<0.05, **<0.01, ***<0.001. (**b**) H&E staining and pathological scoring of colons from *C. rodentium* infected, DT injected and anti-IL-2 treated DEREG or wild type littermates (WT) on day 10 p.i.. Data represent mean ± S.E.M. and are one representative of two individual experiments (n=3 mice per group). *<0.05, **<0.01. Scale bar represents 200 μm. (**c**) FACS plots of colonic $CD11b^{+}CD11c^{-}Ly6G^{high}Ly6C^{int}$ neutrophils 12 days after *C. rodentium* infection. Data display one representative out of 3 individual experiments, each with 3 to 5 mice per group (upper panel). Lower left panel

represents frequencies of colonic $Ly6G^{high}Ly6C^{int}$ neutrophils among $CD11b^{+}CD11c^{-}$ cells in mice from different groups. Data, shown as mean ± S.E.M., represent one representative out of three individual experiments, each with 3 to 5 mice per group. Lower right panel represents total number of neutrophils in the colons of mice from different groups. Data, shown as mean ± S.E.M., display one experiment (n=3 to 5 mice per group). *<0.05, **<0.01, ***<0.001. (**d**) *C. rodentium* burden in colonic feces in mice from different groups. Data are pooled from at least 4 individual experiments, each with 2 to 3 mice per group. Data represent mean. **<0.01, ***<0.001. (**e**) Absolute number of total lamina propria IL-17A producing $CD4^{+}CD3^{+}$ T cells (including both $IL17^{+}IFN\text{-}\gamma^{-}$ and $IL17A^{+}IFN\text{-}\gamma^{+}$) in the colons of mice from different groups. Data, shown as mean ± S.E.M., display one representative of 4 experiments, each with 3 to 5 mice per group.

Figure 1

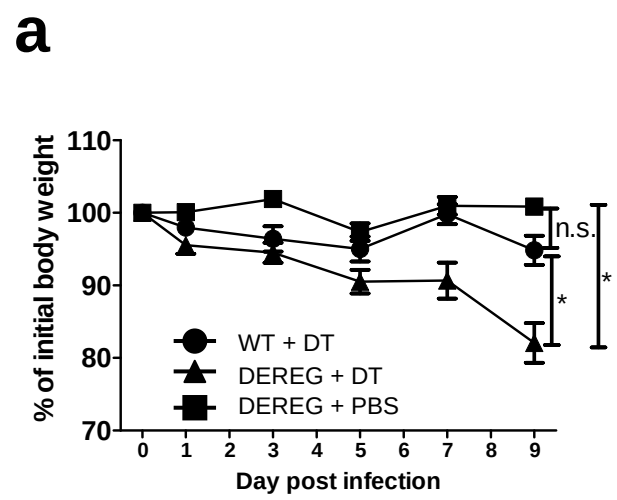
a
% of initial body weight
110
100
90
80
70
0 1 2 3 4 5 6 7 8 9
Day post infection
WT + DT
DEREG + DT
DEREG + PBS
n.s.
*
*

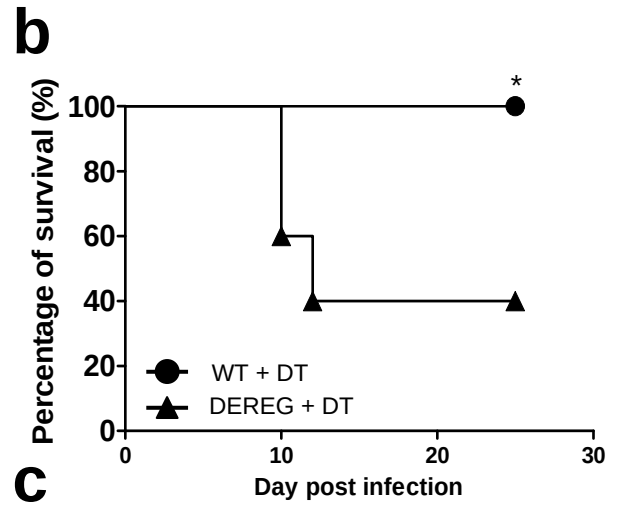
b
Percentage of survival (%)
100
80
60
40
20
0
0 10 20 30
Day post infection
WT + DT
DEREG + DT
*

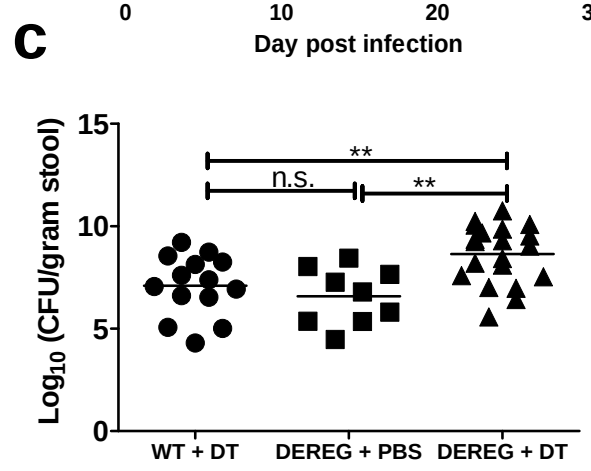
c
Log10 (CFU/gram stool)
15
10
5
0
WT + DT
DEREG + PBS
DEREG + DT
n.s.
**
**

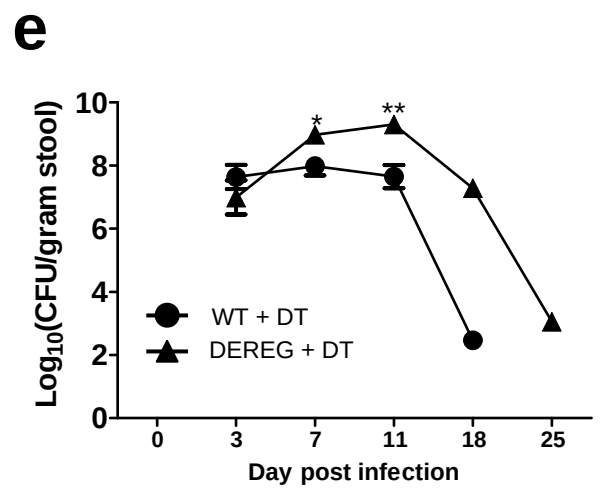
e
Log10(CFU/gram stool)
10
8
6
4
2
0
0 3 7 11 18 25
Day post infection
WT + DT
DEREG + DT
*
**

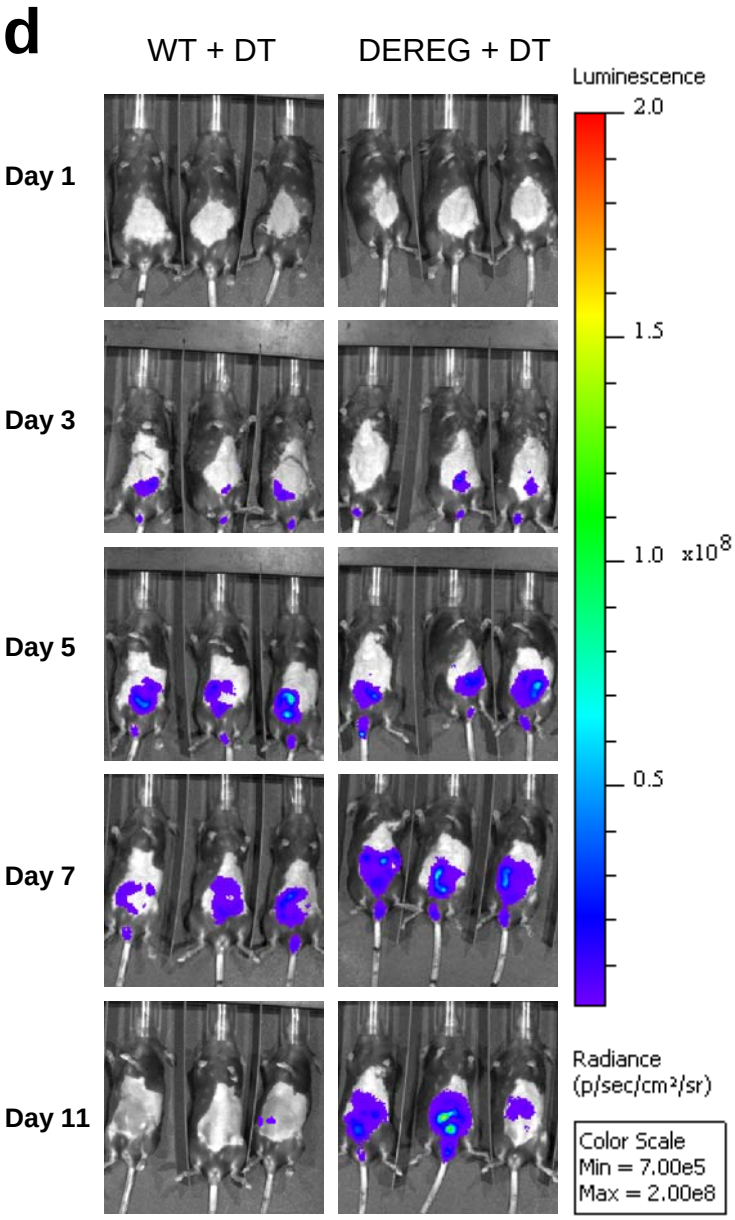
d
WT + DT
DEREG + DT
Luminescence
2.0
1.5
1.0
0.5
x10^8
Day 1
Day 3
Day 5
Day 7
Day 11
Radiance
(p/sec/cm²/sr)
Color Scale
Min = 7.00e5
Max = 2.00e8

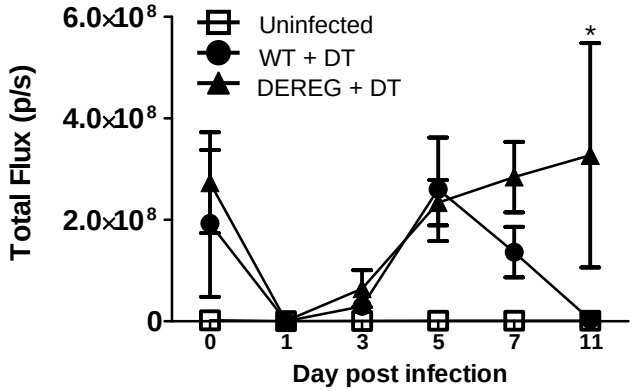
Total Flux (p/s)
6.0x10^8
4.0x10^8
2.0x10^8
0
0 1 3 5 7 11
Day post infection
Uninfected
WT + DT
DEREG + DT
*

Figure 2

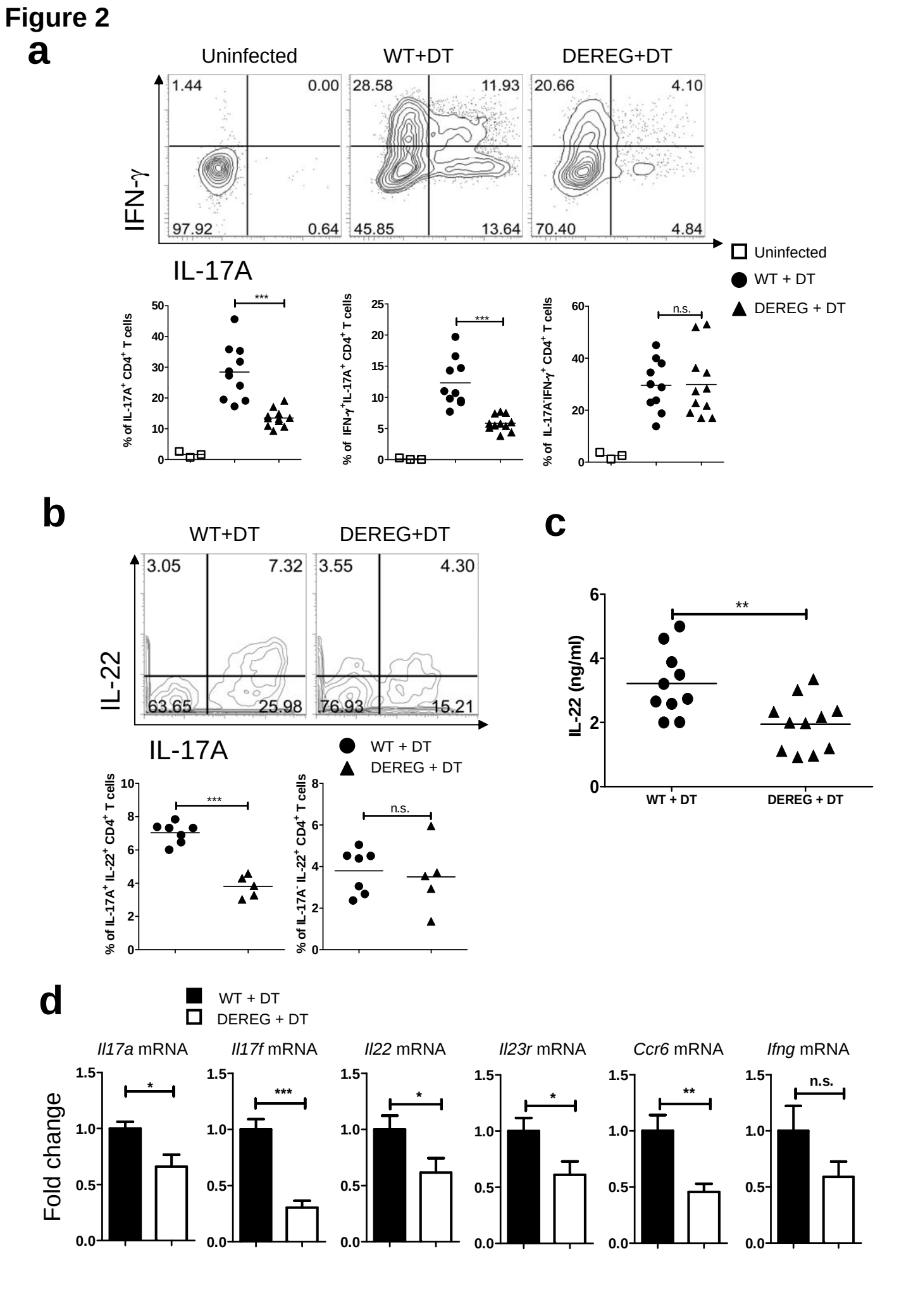
a
Uninfected
WT+DT
DEREG+DT
IFN-γ
1.44
0.00
97.92
0.64
28.58
11.93
45.85
13.64
20.66
4.10
70.40
4.84
IL-17A
Uninfected
WT + DT
DEREG + DT
% of IL-17A+ CD4+ T cells
% of IFN-γ+IL-17A+ CD4+ T cells
% of IL-17A-IFN-γ+ CD4+ T cells
***
n.s.
b
WT+DT
DEREG+DT
IL-22
3.05
7.32
63.65
25.98
3.55
4.30
76.93
15.21
IL-17A
WT + DT
DEREG + DT
% of IL-17A+ IL-22+ CD4+ T cells
% of IL-17A- IL-22+ CD4+ T cells
c
IL-22 (ng/ml)
**
WT + DT
DEREG + DT
d
WT + DT
DEREG + DT
Il17a mRNA
Il17f mRNA
Il22 mRNA
Il23r mRNA
Ccr6 mRNA
Ifng mRNA
Fold change
n.s.

Figure 3

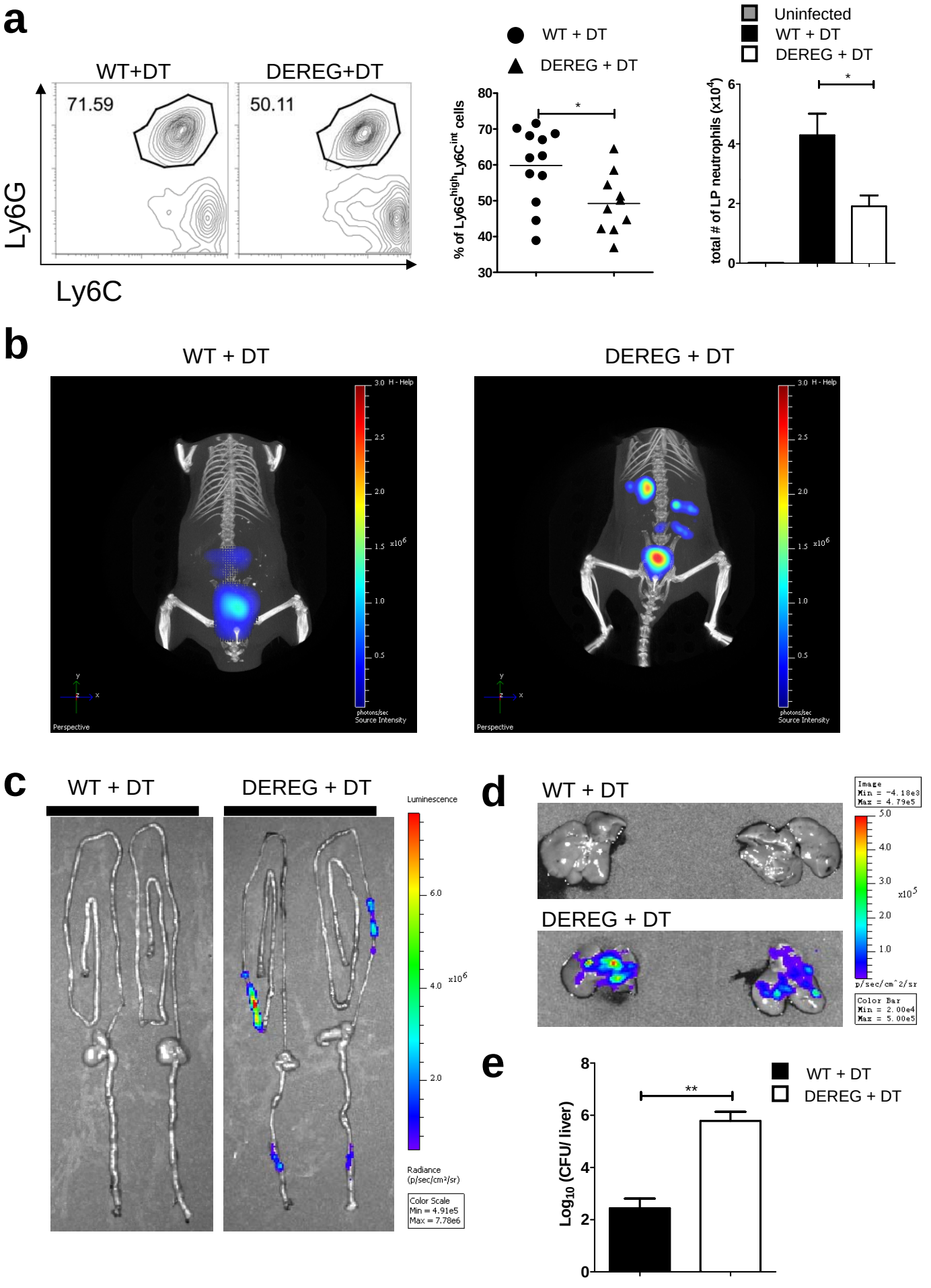
a
WT+DT
DEREG+DT
71.59
50.11
Ly6G
Ly6C
WT + DT
DEREG + DT
% of Ly6G^high Ly6C^int cells
Uninfected
WT + DT
DEREG + DT
total # of LP neutrophils (x10^4)
b
WT + DT
DEREG + DT
Perspective
photons/sec
Source Intensity
c
WT + DT
DEREG + DT
Luminescence
Radiance (p/sec/cm²/sr)
Color Scale
Min = 4.91e5
Max = 7.78e6
d
WT + DT
DEREG + DT
Image
Min = -4.18e3
Max = 4.79e5
p/sec/cm^2/sr
Color Bar
Min = 2.00e4
Max = 5.00e5
e
WT + DT
DEREG + DT
Log10 (CFU/ liver)

Figure 4

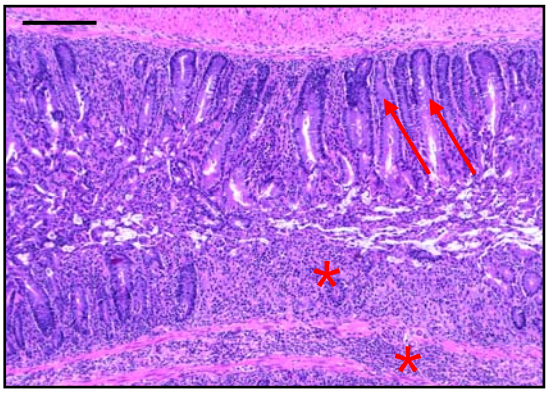

WT + DT

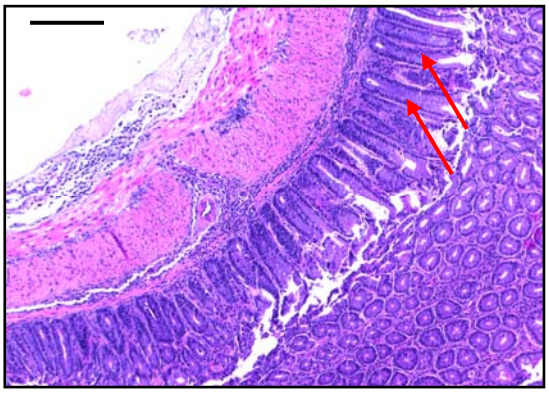

DEREG + DT

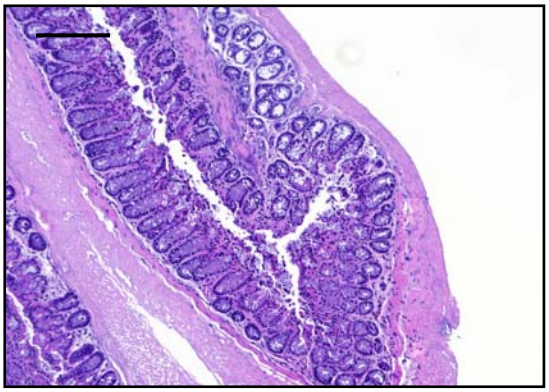

uninfected control

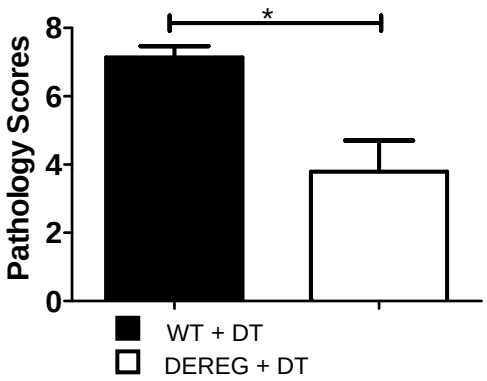

Figure 5

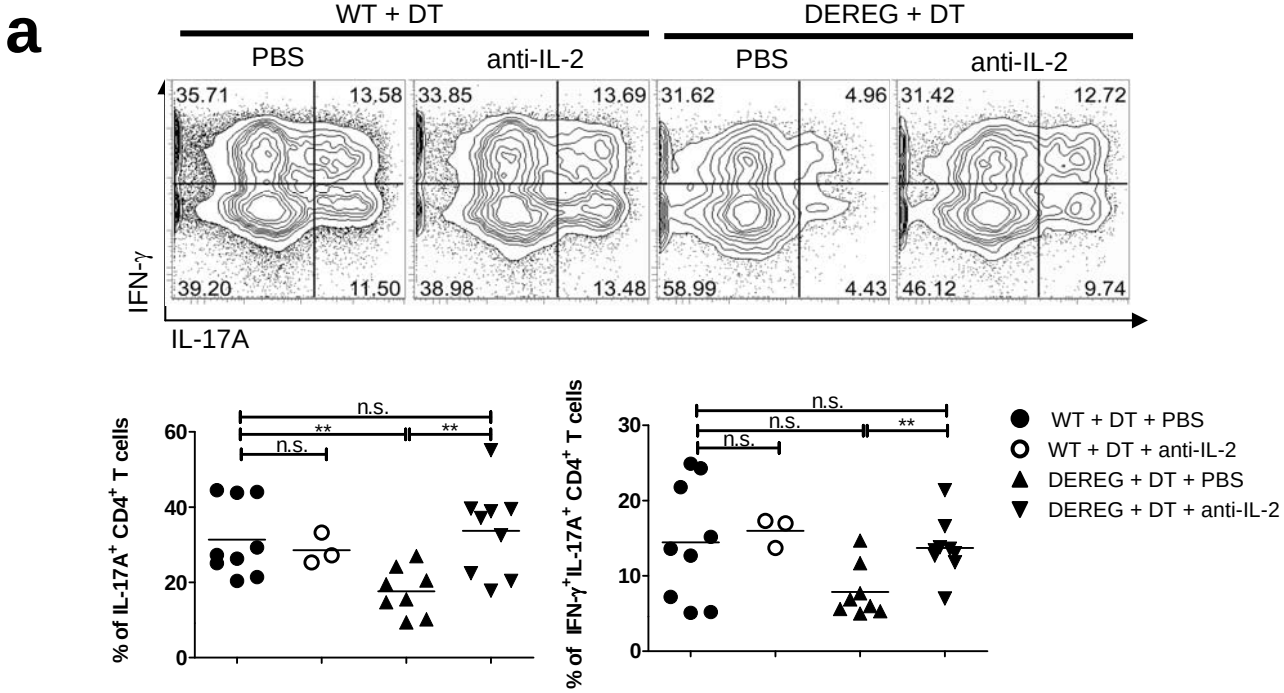
a
WT + DT
DEREG + DT
PBS
anti-IL-2
PBS
anti-IL-2
35.71
13.58
39.20
11.50
33.85
13.69
38.98
13.48
31.62
4.96
58.99
4.43
31.42
12.72
46.12
9.74
IFN-γ
IL-17A
% of IL-17A+ CD4+ T cells
% of IFN-γ+IL-17A+ CD4+ T cells
n.s.
**
WT + DT + PBS
WT + DT + anti-IL-2
DEREG + DT + PBS
DEREG + DT + anti-IL-2

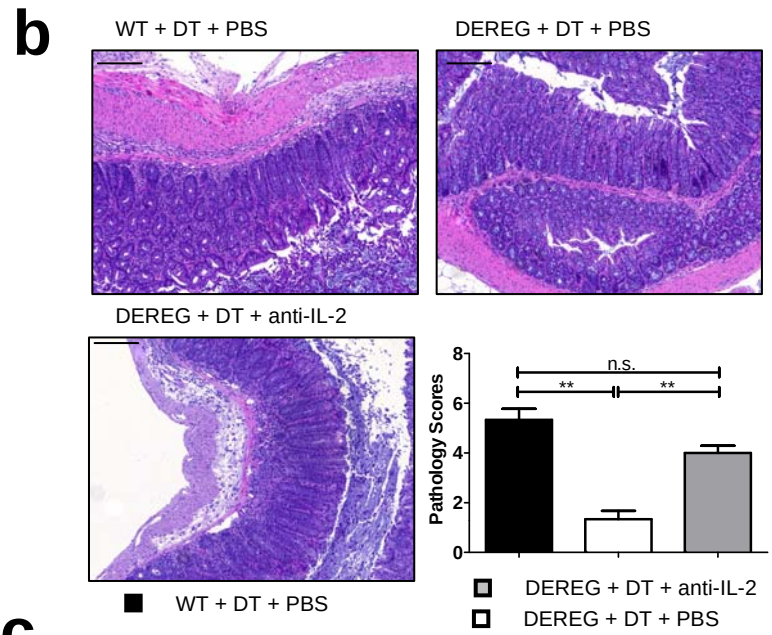
b
WT + DT + PBS
DEREG + DT + PBS
DEREG + DT + anti-IL-2
Pathology Scores
n.s.
**
WT + DT + PBS
DEREG + DT + anti-IL-2
DEREG + DT + PBS

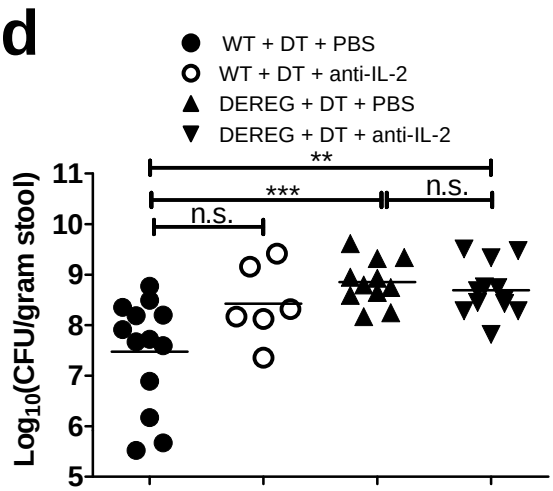
d
WT + DT + PBS
WT + DT + anti-IL-2
DEREG + DT + PBS
DEREG + DT + anti-IL-2
Log10(CFU/gram stool)
**
***
n.s.

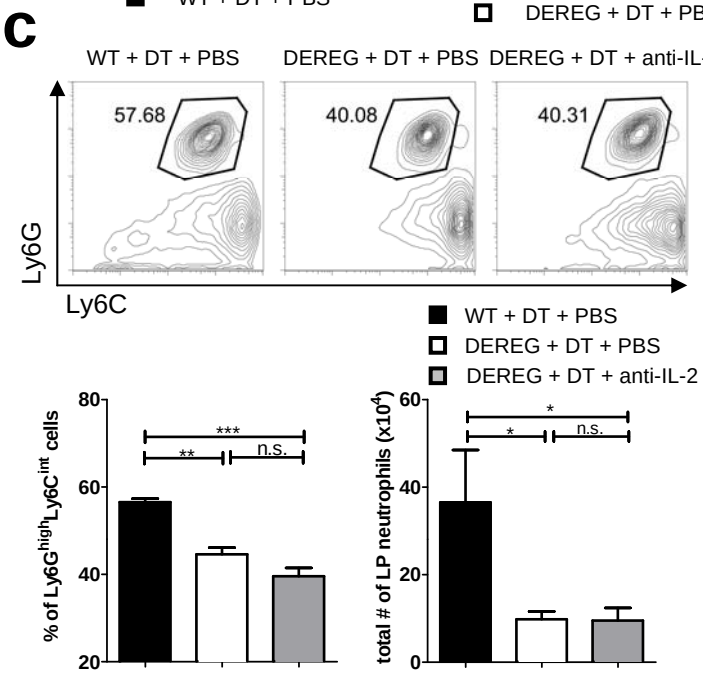
c
WT + DT + PBS
DEREG + DT + PBS
DEREG + DT + anti-IL-2
57.68
40.08
40.31
Ly6G
Ly6C
% of Ly6GhighLy6Cint cells
total # of LP neutrophils (x10⁴)
***
**
*
n.s.

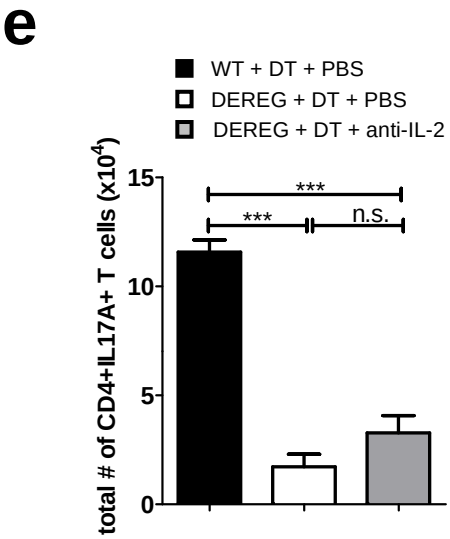
e
WT + DT + PBS
DEREG + DT + PBS
DEREG + DT + anti-IL-2
total # of CD4+IL17A+ T cells (x10⁴)
***
n.s.